VERIFICATION AND VALIDATION OF NEUTRONIC CODES USING THE START-UP FUEL LOAD AND CRITICALITY TESTS PERFORMED IN THE CHINA EXPERIMENTAL FAST REACTOR

ARMANDO GOMEZ-TORRES, ROBERTO LOPEZ-SOLIS, JUAN GALICIA-ARAGÓN
Instituto Nacional de Investigaciones Nucleares (ININ),
Ocoyoacac, La Marquesa, Mexico
Email: armando.gomez@inin.gob.mx

XINGKAI HUO
China Institute of Atomic Energy (CIAE),
Beijing, China

VLADIMIR KRIVENTSEV, CHIRAYU BATRA
International Atomic Energy Agency (IAEA),
Vienna, Austria

T. K. KIM, M. JARRETT
Argonne National Laboratory (ANL),
USA

EMIL FRIDMAN
Helmholtz-Zentrum Dresden-Rossendorf (HZDR),
Germany

YOUQI ZHENG, XIANAN DU
School of Nuclear Science and Technology, Xi'an Jiaotong University (XJTU),
China

J. BODI, K. MIKITYUK
Paul Scherrer Institute (PSI),
Switzerland

DEOKJUNG LEE, TUAN QUOC TRAN, JIWON CHOE
Ulsan National Institute of Science and Technology (UNIST),
Republic of Korea

H. TANINAKA
Japan Atomic Energy Agency (JAEA),
Japan

M. SZOGRADI
Technical Research Centre (VTT),
Finland

P. DARILEK
VUJE,
Slovakia

A. HERNANDEZ-SOLIS, A. STANKOVSKIY, G. VAN DEN EYNDE
Belgian Nuclear Centre (SCK-CEN),
Belgium

IULIANA ELENA VISAN, ANDREEA MOISE
Institute for Nuclear Research (RATEN),
Pitești, Romania.

VALERIO GIUSTI
Dipartimento di Ingegneria Civile ed Industriale (DICI), Università di Pisa,
Italy

ALESSANDRO PETRUZZI, DI PASQUALE SIMONE
Nuclear and Industrial Engineering (N.IN.E.),
Lucca, Italy

Abstract

Under the framework of coordinated research activities of the International Atomic Energy Agency (IAEA), the China Institute of Atomic Energy (CIAE) proposed a coordinated research project (CRP) to develop a benchmark based on the start-up tests of the China Experimental Fast Reactor (CEFR). 29 international organizations from 17 countries are participating in this CRP. Among the different physical start-up tests conducted in 2010 in the CEFR, the fuel loading and criticality experimental data is included. Before the start-up of the reactor, the core was preliminarily loaded with mock-up fuel sub-assemblies (SAs) in the active fuel positions. The reactor reached first criticality by replacing these mock-up SAs with real fuel SAs step by step. In a sub-critical extrapolation process, the number of fuel SAs to be loaded is determined by extrapolation of reciprocal of count rate and following safety requirements. As the reactor core approaches to criticality, the subcritical extrapolation ended and the next process is called super-critical extrapolation, which uses the control rods to reach criticality by period method. For the CEFR, the final clean-core criticality state was reached with 72 fuel SAs and the regulating control rod at the position of 70mm with a measured sodium temperature of 245℃. In the paper, the main results of the contributing international organizations for the fuel loading process in the blind and refined phase are summarized and compared with the experimental data. Additionally, code to code comparisons for normalized radial power are also presented. In general, results from all institutions show very good agreement while comparing with the experimental data. The results are divided in deterministic and stochastic codes and in each case, discussion and deep analysis is presented.

1. INTRODUCTION

China Experimental Fast Reactor (CEFR) is a 65MWth pool-type sodium-cooled fast-spectrum reactor, it is located in the China Institute of Atomic Energy (CIAE) and it is the first fast reactor of China, which reached first criticality in 2010. In the physical start-up tests in 2010, four series of experiments were conducted, including fuel loading and criticality, measurement of control rod worth, measurement of reactivity coefficients, and foil activation measurements. These experiments not only made an essential part of the reactor start-up, but also produced valuable data for the validation of core design, numerical code and nuclear data. Under the direction and support from International Atomic Energy Agency (IAEA), CIAE proposed a coordinated research project (CRP) to develop a benchmark based on the start-up tests. Under the CRP framework, 29 international organizations from 17 countries are participating in this CRP.

Among the different physical start-up tests conducted in 2010 in the CEFR, the fuel loading and criticality experimental data is included. In the paper, a brief description of the CEFR and, in particular, of the fuel load criticality experiment are presented followed by the main results of the contributing international organizations for the fuel loading process in the blind and refined phase. Comparisons with the experimental data and some code to code comparisons for normalized radial power are also presented.

2. CEFR BRIEF DESCRIPTION

The core of first loading consists of 79 fuel subassemblies (SA), 8 control SAs, one neutron source SA, 394 stainless steel (SS) SAs, and 230 boron shielding SAs. The 2 SS SAs in the fuel region, which are used to compensate for the residual reactivity of the fresh fuel in the first loading, will be replaced by 2 fuel SAs in the equilibrium refuelling cycle; at the border of the boron shielding SAs there is an in-core spent fuel storage area, which can hold 56 spent fuel SAs; however, in the first loading, there is no spent fuel SA and the storage area were loaded with 56 Type-IV SS SAs; therefore, in the loading of each equilibrium refuelling cycle there are 81 fuel SAs and 336 SS SAs. The main parameters of the CEFR and a detailed description of each component can be found in [1].

3. FUEL LOAD AND CRITICALITY TEST

Before the start-up of the reactor, the core was preliminarily loaded with mock-up fuel sub-assemblies (SAs) in the active fuel positions. The reactor reached first criticality by replacing these mock-up SAs with real fuel SAs step by step. In a sub-critical extrapolation process, the number of fuel SAs to be loaded is determined by extrapolation of reciprocal of count rate and following safety requirements, the process is shown in Fig. 1. As the reactor core approaches to criticality, the subcritical extrapolation ended and the next process is called super-critical extrapolation, which uses the control rods to reach criticality by period method. In the super-critical extrapolation, 72 fuel SA were loaded. Control rods with exception of one regulating rod that is fully inserted, were totally withdrawn to out-of-core position. The regulating control rod is then withdrawn step by step to three different positions to reach super-criticality. At each position, a positive period was obtained. Based on that, the critical position of control rod is predicted by extrapolation (based on the calculated control rod worth curve). Finally, the control rod is put to the predicted critical position, and the reactor clean-core criticality state is reached. For the CEFR, the final clean-core criticality state was reached with 72 fuel SAs and the regulating control rod at the position of 70 mm with a measured sodium temperature of 245℃. Three start-up detectors located near the active core (temporarily installed) were used to get the count rate throughout the criticality approaching process.

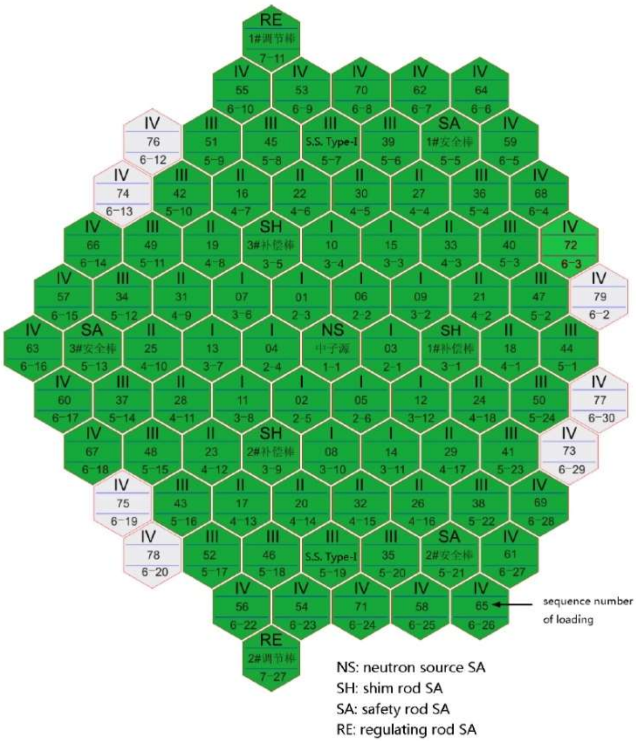

FIG. 1. LOADING CONFIGURATION OF THE CLEAN CORE

3.1. Expected and optional output and experimental results for the fuel load and criticality test

Table 1 shows the expected and optional output for this test. The first output is the k_{eff} when 71 fuel rods were loaded, and all the control rods were out-of-core. The second one is the k_{eff} with RE2 at critical position. Theoretically, the k_{eff} must be 1.0 for critical state; however, the core is not exactly critical in experiment. The main reason is that the final critical position of RE2 was obtained through not only the previous three positive periods but also the calculated worth curve of RE2 rod. Important is to notice that the predicted critical position is possibly deviated from the actual critical position due to the possible errors of measurement and calculation. Three supercritical states with control rod position RE2 at 190, 170 and 151 mm are also to be reported.

In addition, as a code to code comparisons exercise, in the CRP the fuel loading process before the 10th loading step (or subcritical process) was also considered and some organizations presented alternative output of the k_{eff} of each fuel loading step. The core layout of these steps is the one shown in Fig. 1, referring to the sequence numbers of loading. Furthermore, another optional output was defined to account for local effects in the axial-averaged normalized power at the path shown in Figure 2. Table 2 presents the ID of each fuel subassembly. The normalization is done with the arithmetic average of the 5 values of each subassembly, i.e., the normalization factor is the sum of them divided by 5.

TABLE 1. EXPECTED AND OPTIONAL OUTPUT OF EXPERIMENT

Number of fuel SAs loaded	Rod position/mm		Core state	Expected output
	Other 7 control rods	RE2 position [mm]		
71	Out-of-core	Out-of-core	End of subcritical process	k-eff
72	Out-of-core	190	Supercritical	k-eff
72	Out-of-core	170	Supercritical	k-eff
72	Out-of-core	151	Supercritical	k-eff
72	Out-of-core	70	Critical (Predicted)	k-eff
24, 40*, 46, 55, 61, 65, 68, 69, 70	Out-of-core	Out-of-core	Subcritical	k-eff

* After the loading of the 40th fuel SA, two SS SAs are loaded

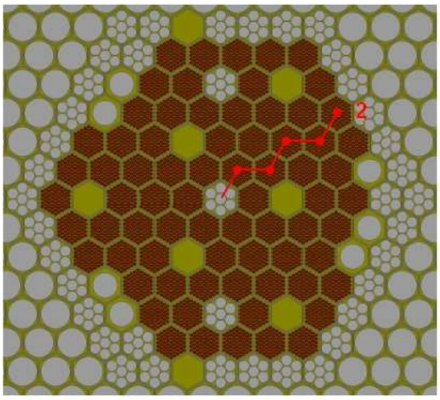

FIG. 2. PATH FOR NORMALIZED POWER CALCULATION

TABLE 2. ID OF FUEL SA’S IN CALCULATION PATH

Point	Assembly
1	I-06
2	I-09
3	II-33
4	III-40
5	IV-68

3.2. Experimental results for the fuel load and criticality test

Table 3 shows the experimental results for the expected calculations in terms of reactivity with an estimated value of 0.0 in the final critical position. Since calculations with codes provide directly k_{eff}, following equation was used to report in each case reactivity.

$$\rho = (k_{eff} - 1.0)/k_{eff} \tag{1}$$

Furthermore, in each case simple deviation from experiment and reactivity ($\rho_{exp} - \rho_{cal}$) from calculation was calculated. Since experimental data is only available for the 4 final values of expected output, given in Table 3, refined calculations are compared only for these 4 cases with deterministic and stochastic codes.

TABLE 3. EXPERIMENTAL RESULTS FOR THE EXPECTED CALCULATIONS

RE2 position [mm]	$\rho\ (\frac{\Delta k}{k})$	$\rho\ (\frac{\Delta k}{k})$ [pcm]
190	3.95E-04	40
170	3.35E-04	34
151	2.45E-04	25
70	0.0 Estimated	0

4. PARTICIPATING INSTITUTIONS

The participants were divided in two groups, the ones using deterministic codes enlisted in Table 4 and the ones using stochastic codes which details are presented in Table 5. Not all of them participated in both phases: blind and refined but tables include all the participants independent from phase.

TABLE 4. PARTICIPANTS WITH DETERMINISTIC CODES

Country	**Institute**	**XS**	**Nodal Code**	**Lattice Code**
China	**CIAE**: China Institute of Atomic Energy	ENDFB/VIII.0	NAS	PASC
China	**XJTU**: Xi'an Jiaotong University	ENDF/B-VII.0	SARAX-LAVENDER v1.5	SARAX-TULIP v1.5
France	**CEA**: Commissariat à l'Énergie Atomique	JEFF 3.1, JEFF 3.1.1	ERANOS, APOLLO3	ERANOS, APOLLO3
Germany	**GRS**: Gesellschaft für Anlagen- und Reaktorsicherheit	ENDF/B-VII.0	FENNECS	Serpent 2.1.31
Germany	**KIT**: Karlsruhe Institute of Technology	JEFF.3.1	VARIANT	ECCO
Hungary	**CER**: Centre for Energy Research	ENDFB/VIII.0	KIKO3DMG	Serpent 2.1.31
India	**IGCAR**: Indira Gandhi Centre for Atomic Research	ABBN-93, ERALIB-1 JEF-2.2	FARCOB, ERANOS	FARCOB, ERANOS
Japan	**JAEA**: Japan Atomic Energy Agency	JENDL-4.0	DIF3D10.0/PARTISN5.97	SLAROM-UF
Korea	**KAERI**: Korea Atomic Energy Research Institute	ENDF/B-V.II.0	DIF3D-VARIANT 11.0	MC2-3
Korea	**UNIST**: Ulsan National Institute of Science and Technology	ENDF/B-VII.1	RAST-K	MCS
Mexico	**ININ**: Instituto Nacional de Investigaciones Nucleares	ENDFB/VIII.0	AZNHEX (SPL)	Serpent 2.1.31
Russia	**NRCKI**: National Research Center: Kurchatov Institute	ABBN-93	JARFR	JARFR
Russia	**SSL:** Simulation Systems Ltd.	ENDFB/VII	DYNCO	WIMSD4
Switzerland	**PSI**: Paul Scherrer Institut	JEFF 3.1.1	PARCS v27	Serpent 2.1.30
UK	**UoC**: University of Cambridge	JEFF3.1.2	WIMS 11	WIMS 11
Ukraine	**KIPT**: Kharkov Institute of Physics & Technology	BNAB-76	FANTENS-2	
USA	**ANL**: Argonne National Laboratory	ENDF-B/VII.0	MCC-3, DIF3D	MCC-3

TABLE 5. PARTICIPANTS WITH STOCHASTIC CODES

Country	Institute	XS	Code
Belgium	**SCK-CEN**: Belgian nuclear research centre	ENDF/B-VII.1	OpenMC 0.10.0
China	**CIAE:** China Institute of Atomic Energy	ENDFB/VIII.0	RMC
China	**INEST**: Institute of Nuclear Energy Safety Technology	HENDL3.0	SuperMC
Finland	**VTT**: Technical Research Centre of Finland	ENDF-B/VII.0, JEFF 3.1.2	Serpent 2.1.31
France	**CEA**: Commissariat à l'Énergie Atomique	JEFF3.1.1	TRIPOLI4
Germany	**HZDR**: Helmholtz Zentrum DresdenRossendorf	JEFF-3.1, JEFF-3.3, ENDF/B-VII.1, ENDF/B-VIII.0	Serpent 2.1.31
Germany	**GRS:** Gesellschaft für Anlagen- und Reaktorsicherheit	ENDF/B-VII.1	Serpent 2.1.30
Hungary	**CER**: Centre for Energy Research	ENDFB/VIII.0	Serpent 2.1.31
IAEA	**IAEA**: International Atomic Energy Agency	ENDF/B-VII.1	OpenMC, Serpent 2.1.27
India	**IGCAR**: Indira Gandhi Centre for Atomic Research	ENDF/B VIII.0, JEFF 3.3, JENDL 4.0, ROSFOND 2010, CENDL 3, TENDL 2017	OpenMC 0.10.0
Italy	**NINE-UNIPI**: Nuclear and Industrial Engineering-Università di Pisa	ENDFB/VIII.0	Serpent 2.1.31
Japan	**JAEA**: Japan Atomic Energy Agency	JENDL-4.0	MVP-II
Korea	**KAERI**: Korea Atomic Energy Research Institute	ENDF/B-VII.1	McCARD
Korea	**UNIST**: Ulsan National Institute of Science and Technology	ENDF/B-VII.1	MCS
Mexico	**ININ**: Instituto Nacional de Investigaciones Nucleares	ENDFB/VIII.0	Serpent 2.1.30
Romania	**RATEN**: Institute for Nuclear Research	ENDFB/VIII.0	Serpent 2.1.31, MCNP 6.1
Russia	**IPPE**: Institute of Physics and Power Engineering	ROSFOND10+	MMKC
Russia	**NRCKI**: National Research Center: Kurchatov Institute	JEFF-3.3	Serpent 2.1.31, MCNP
Slovakia	**VUJE**:	ENDF/B-VII.1	Serpent 2.1.31
USA	**NRC**: Nuclear Regulatory Commission	ENDF/B-VII.1	Serpent 2.1.30

5. RESULTS

5.1. Blind phase calculations

First of all, calculations were performed in blind, i.e., experimental data were not available for participants. In the following subsections, results for deterministic and stochastic codes will be presented in the blind phase and since no experimental data were available, comparisons are presented against average value of all participants.

5.1.1. Deterministic codes

For the deterministic cases, in Figures 3 and 4 results for the expected output and optional output are presented as well as the average value of all participants in black line. In general, most of the deterministic results remained subcritical even in the steps when a slightly super criticality state was expected. Deviations from average value ranged in [-900 to1,000] pcm. Average of absolute value of deviation (from average value) of all participant was 484 pcms. As expected, higher differences were found in codes based on diffusion approximation. Table 6 shows the results obtained for normalized power exercise together with the deviation from average value.

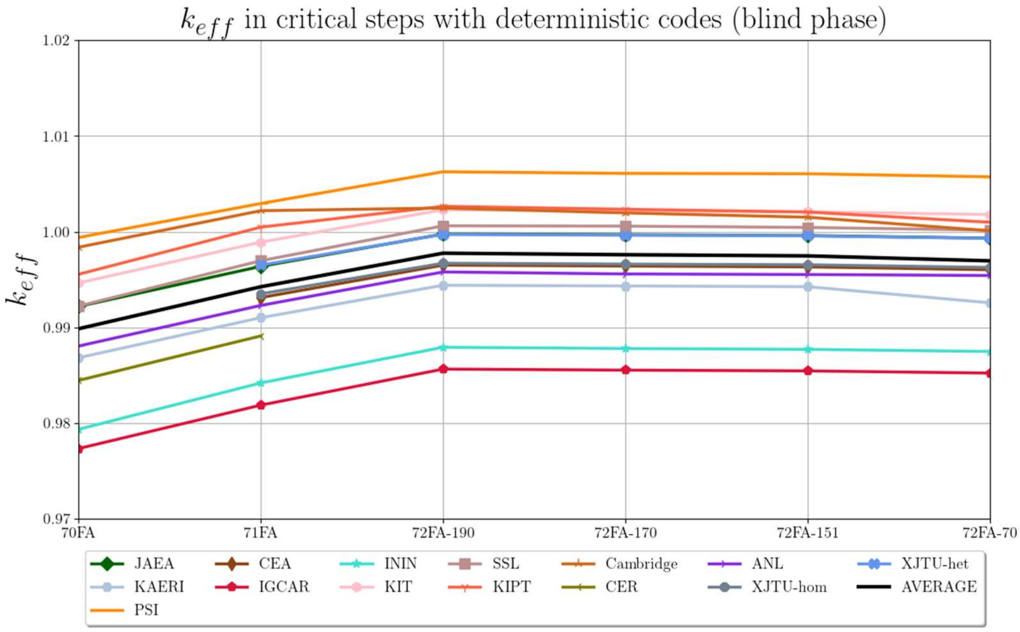

FIGURE 3. EXPECTED OUTPUT WITH DETERMINISTIC CODES IN THE BLIND PHASE

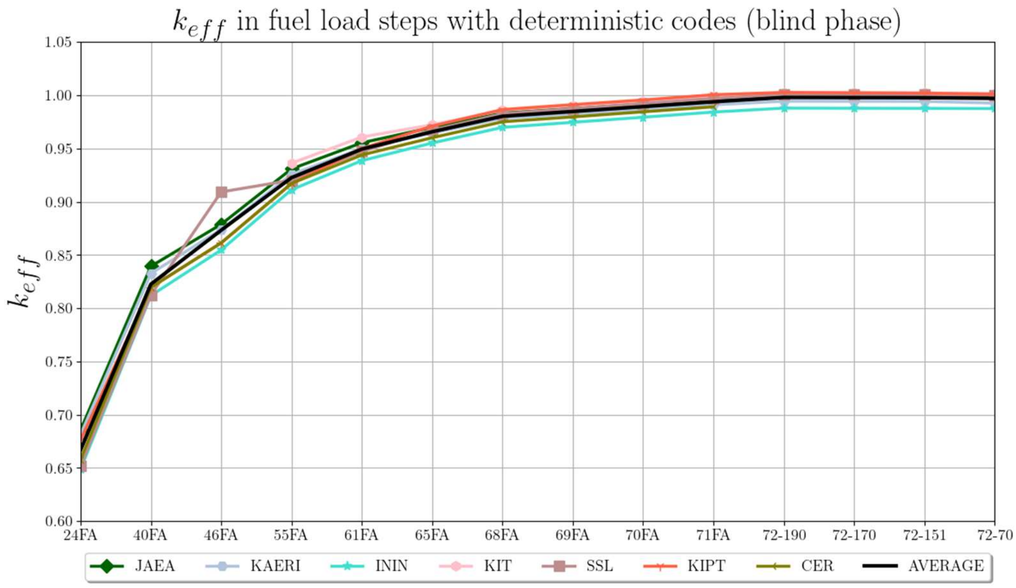

FIGURE 4. OPTIONAL OUTPUT WITH DETERMINISTIC CODES IN THE BLIND PHASE

TABLE 6. NORMALIZED POWER VALUES AND DEVIATION FROM AVERAGE VALUE

Fuel SA	**I-06**		**I-09**		**II-33**		**III-40**		**IV-68**	
	Value	**Dev(%)**	**Value**	**Dev(%)**	**Value**	**Dev(%)**	**Value**	**Dev(%)**	**Value**	**Dev(%)**
Average	**1.14654**		**1.10129**		**1.02453**		**0.93199**		**0.82340**	
KAERI	1.14825	-0.15	1.09960	0.15	1.01813	0.62	0.91719	1.59	0.81683	0.80
PSI	1.21179	-5.69	1.14945	-4.37	1.02547	-0.09	0.89232	4.26	0.72097	12.44
ININ	1.16514	-1.62	1.11009	-0.80	1.02752	-0.29	0.91743	1.56	0.77982	5.29
SSL	1.06100	7.46	1.04600	5.02	1.02700	-0.24	1.00100	-7.41	0.97600	-18.53

5.1.2. Stochastic codes

Since some institutions delivered several results changing either Cross Sections data base, solver or homogenization and heterogenization approach, before presenting results, it is important to describe the main considerations in each case:

- IAEA: the different cases numbered from 1 to 5 stand for: cases 1 and 2 used the Monte Carlo code Serpent with a homogeneous model in which the material in assembly is homogenized radially. Axial mesh is divided by axial material composition and thermal expansion is not applied. Case 1 used ENDF/B-VII.0 and case 2 ENDF/B-VII.1. Case 3 was calculated with OpenMC and ENDF/B-VII.1 and the whole core with heterogenous model. Finally, cases 4 and 5 used Serpent with heterogeneous model, ENDF/B-VII.1 and with the difference that in case 4 the spiral wire is smeared into the coolant region meanwhile in case 5, the cladding thickness is increased to conserve area of spiral wire.
- RATEN presented two calculations: case 1 with Serpent and case 2 with MCNPX 6.2 both with ENDF/B-VIII.0.
- IGCAR delivered calculations with OpenMC but case 1 using ENDF/B-VIII.0 and case 2 using JEFF 3.3.
- NRCKI contributed with calculations using MCNP for the case 1 and with Serpent for the case 2, the two of them with JEFF 3.3.

Figures 5 and 6 show the results respectively for expected and optional output in the k_{eff} exercises. As in the deterministic case, average value of all participants is shown in black line.

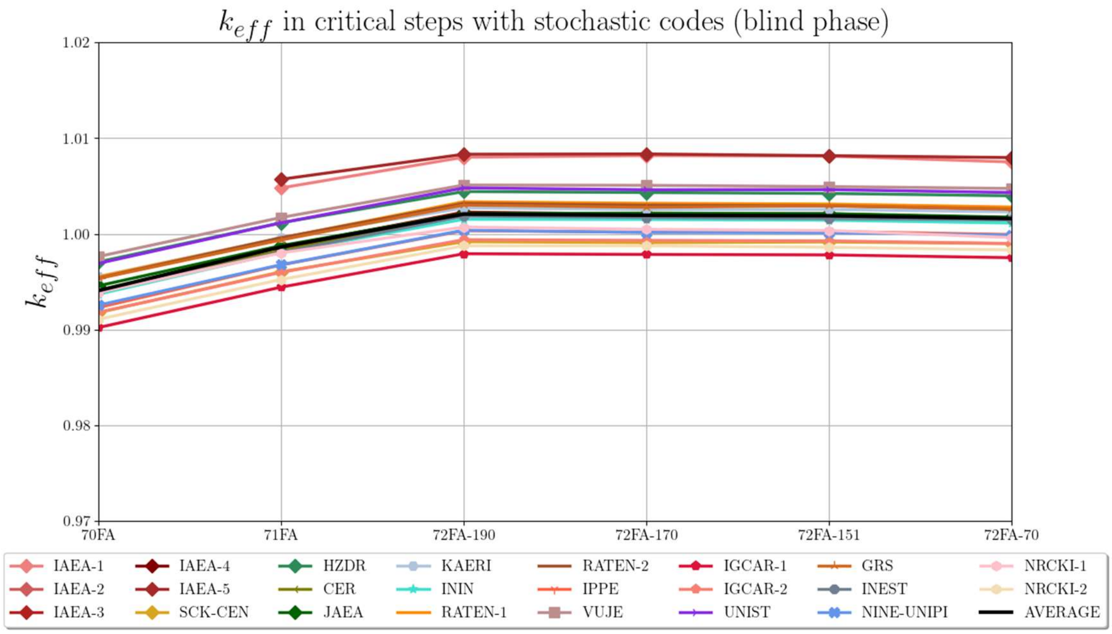

FIGURE 5. EXPECTED OUTPUT WITH STOCHASTIC CODES IN THE BLIND PHASE

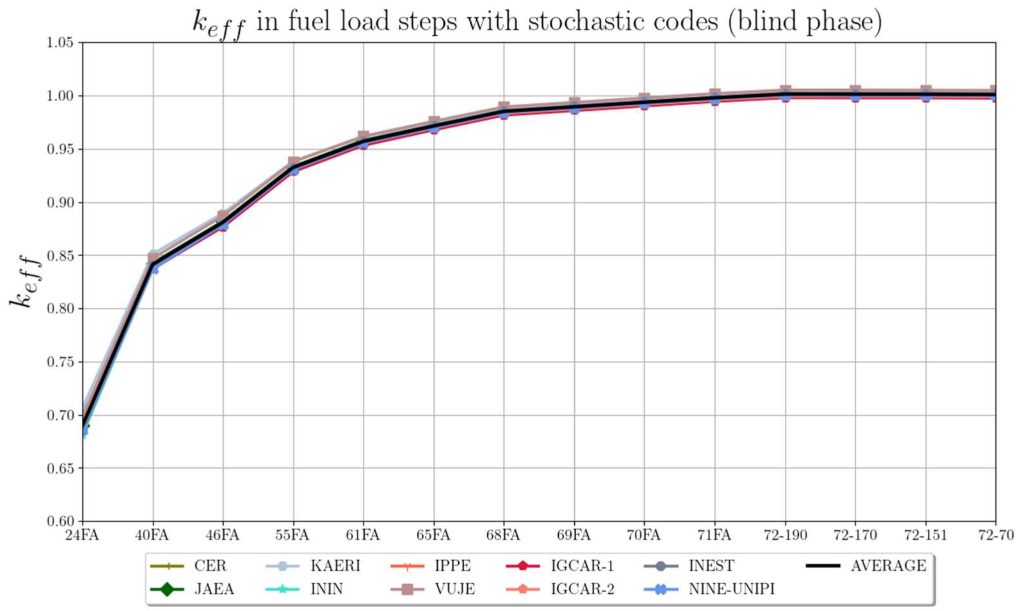

FIGURE 6. OPTIONAL OUTPUT WITH STOCHASTIC CODES IN THE BLIND PHASE

As expected, in the case of stochastic codes, deviation from average value was significantly lower than with deterministic codes, since all Monte Carlo codes have the same foundations. The deviation in pcm from average values ranked in ±400 pcm with just some exceptions with over 600 pcm as an absolute value for the homogeneous models. For the normalized power exercise, Table 7 presents the results of each participant compared against the averaged value. In this case deviation from averaged value remain below the 1% in absolute value with exception of IAEA-1 case in which deviations are over 1% due to the homogenization.

TABLE 7 NORMALIZED POWER VALUES AND DEVIATION IN PERCENT FROM AVERAGE VALUE

Fuel SA	**I-06**		**I-09**		**II-33**		**III-40**		**IV-68**	
	Value	**Dev (%)**	**Value**	**Dev (%)**	**Value**	**Dev (%)**	**Value**	**Dev (%)**	**Value**	**Dev (%)**
Average	**1.1430**		**1.0992**		**1.0175**		**0.9211**		**0.8192**	
RATEN-1	1.1483	-0.46	1.1016	-0.22	1.0210	-0.35	0.9181	0.32	0.8110	1.01
ININ	1.1488	-0.50	1.1017	-0.23	1.0205	-0.30	0.9159	0.57	0.8131	0.75
SCK-CEN	1.1479	-0.43	1.1014	-0.20	1.0198	-0.23	0.9183	0.30	0.8126	0.81
IAEA-1	1.1699	-2.35	1.1214	-2.02	1.0291	-1.14	0.8959	2.73	0.7837	4.34
IAEA-2	1.1520	-0.79	1.1042	-0.46	1.0133	0.41	0.9158	0.57	0.8146	0.57
IAEA-3	1.1530	-0.87	1.1042	-0.46	1.0133	0.41	0.9149	0.67	0.8146	0.57
IAEA-4	1.1518	-0.77	1.1031	-0.36	1.0141	0.34	0.9157	0.59	0.8154	0.47
IAEA-5	1.1460	-0.26	1.0990	0.01	1.0126	0.48	0.9187	0.26	0.8238	-0.55
UNIST	1.1531	-0.88	1.0909	0.75	1.0241	-0.66	0.9193	0.20	0.8126	0.81
KAERI	1.1499	-0.60	1.1034	-0.39	1.0177	-0.03	0.9185	0.28	0.8105	1.07
NINE-UNIPI	1.1490	-0.52	1.1032	-0.37	1.0201	-0.25	0.9175	0.38	0.8103	1.10
NRCKI-1	1.0410	8.93	1.0520	4.29	1.0012	1.60	0.9876	-7.22	0.9182	-12.08
NRCKI-2	1.1489	-0.51	1.1029	-0.34	1.0202	-0.27	0.9180	0.34	0.8100	1.13

5.2. Refined phase calculations

Since experimental data is only available for the 4 final values of expected output, given in Table 3, refined calculations are compared only for these 4 cases with deterministic and stochastic codes.

5.2.3. Deterministic codes

For the refined phase, some institutions provided results with different codes and/or approaches, as follows:

- CEA that delivered results with ERANOS (CEA-1) and APOLLO3 (CEA-2).
- IGCAR reported results with code FARCOB (IGCAR-1) and code ERANOS (IGCAR-2).
- ININ used same code AZNHEX but with different Simplified Spherical Harmonics approach: SP_3 (ININ-1) and SP_7 (ININ-2).
- ANL used code MCC-3 (ANL-1) and DIF3D (ANL-2).

The reactivity values from k_{eff} calculations were obtained by means of Eq. 1. Table 8 show reactivity values for each participant and respective deviation from experimental value. Additionally, Figure 7 shows same results but in k_{eff} values. In this refined phase, significant improvement was obtained in calculations. Average of absolute value of deviation from all participant was only 320 pcm's.

TABLE 8 CALCULATED REACTIVITY VALUES AND DEVIATION IN PCM FROM DETERMINISTIC CALCULATIONS AND EXPERIMENTAL DATA

FA CR	**72 190mm**	**Dev (pcm)**	**72 170mm**	**Dev (pcm)**	**72 151mm**	**Dev (pcm)**	**72 70mm**	**Dev (pcm)**
Exp.	**40.0**		**34.0**		**25.0**		**0.0**	
XJTU	150.2	-110	142.1	-108	135.1	-110	110.7	-111
CEA-1	-475.2	515	-484.3	518	-492.4	517	-523.7	524
CEA-2	732.6	-693	724.3	-690	716.8	-692	689.7	-690
GRS	145.8	-106	136.8	-103	117.9	-93	99.9	-100
CER	114.8	-75	107.2	-73	102.7	-78	79.2	-79
IGCAR-1	-164.3	204	-175.5	210	-183.0	208	-206.7	207
IGCAR-2	-204.1	244	-210.9	245	-215.4	240	-233.2	233
JAEA	-24.6	65	-32.9	67	-40.6	66	-67.7	68
KAERI	70.0	-30	62.4	-28	55.1	-30	30.10	-30
UNIST	122.9	-83	114.9	-81	107.3	-82	81.0	-81
ININ-1	437.9	-398	423.6	-390	422.6	-398	398.9	-399
ININ-2	-41.9	82	-56.0	90	-56.7	82	-79.9	80
NRCKI	-728.9	769	-713.5	748	-717.2	742	-705.6	706
PSI	622.1	-582	605.3	-571	601.4	-576	569.7	-570
UoC	246.4	-206	195.6	-162	150.8	-126	8.9	-9
ANL-1	-423.2	463	-443.8	478	-444.6	470	-455.3	455
ANL-2	-66.6	107	-75.1	109	-84.5	110	-110.6	111
CIAE	-1009.0	1049	-1016.2	1050	-1023.4	1048	-1041.7	1042
KIPT	264.3	-224	233.4	-199	204.7	-180	98.3	-98

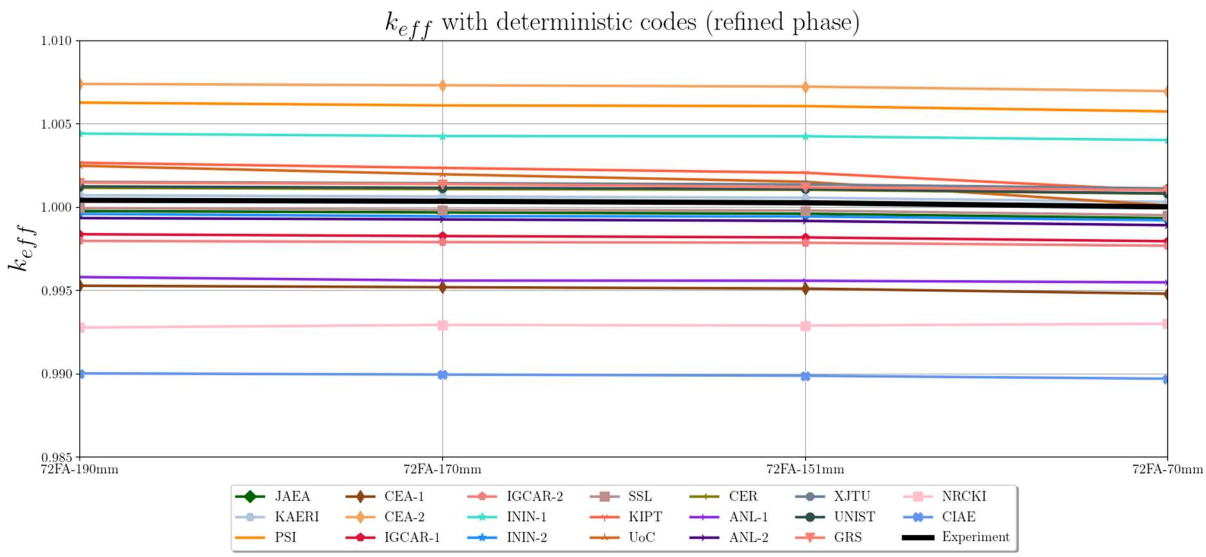

FIGURE 7. EXPERIMENTAL VALUES AND EXPECTED OUTPUT WITH DETERMINISTIC CODES IN THE REFINED PHASE

5.2.4. Stochastic codes

As in the blind phase, several institutions delivered results with different XS's data files as described hereafter:

- VTT used Serpent code with ENDF-B/VII.0 (VTT-1) and JEFF3.1.2 (VTT-2).
- HZDR used Serpent code with JEFF3.1 (HZDR-1), JEFF3.3 (HZDR-2), ENDF-B/VII.1 (HZDR-3) and ENDF-B/VIII.0 (HZDR-4).
- IAEA provided calculations with OpenMC (IAEA-1) and Serpent (IAEA-2).
- IGCAR provided full results with OpenMC using ENDF-B/VIII.0 (IGCAR-1) and JEFF3.3 (IGCAR-2). Furthermore, provided just k_{eff} for the critical position with JENDL (IGCAR-3), ROSFOND (IGCAR-4), CENDL (IGCAR-5), TENDL (IGCAR-6).
- RATEN used ENDF-B/VIII.0 with Serpent (RATEN-1) and MCNP6.1 (RATEN-2).
- NRCKI used JEFF3.3 with Serpent (NRCKI-1) and MCNP6.1 (NRCKI-2).

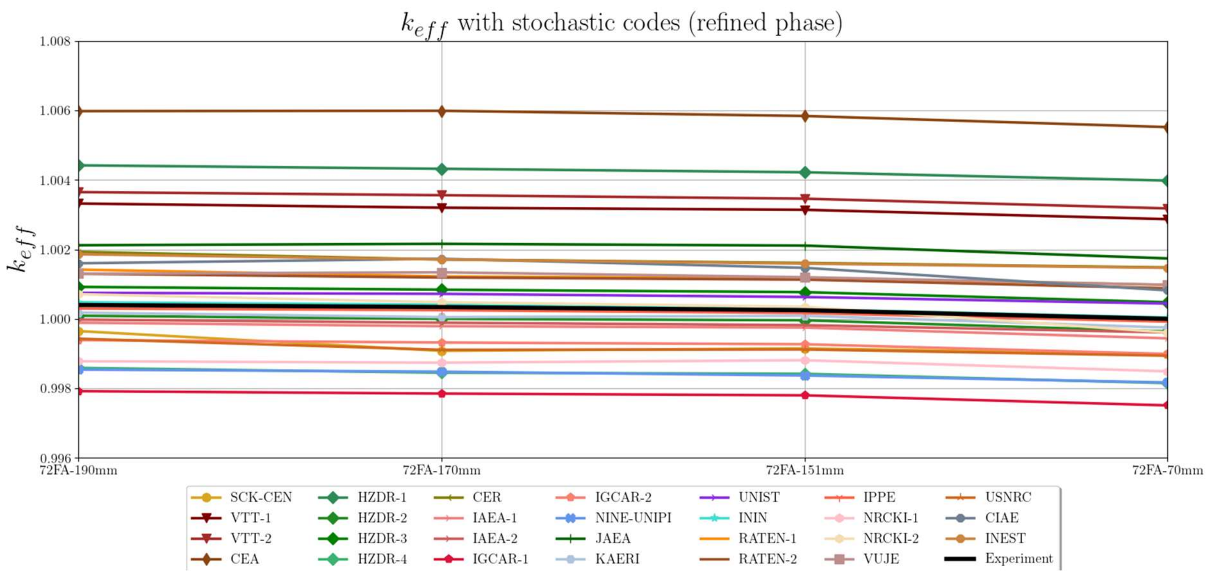

FIGURE 8. EXPERIMENTAL VALUES AND EXPECTED OUTPUT WITH STOCHASTIC CODES IN THE REFINED PHASE

In Figure 8 results for k_{eff} values are presented. In this refined phase, significant improvement was obtained in calculations. Average of absolute value of deviation from experiment of all participants was only 167 pcm. Reactivity values from k_{eff} calculations are reported in Table 9 with the respective deviation from experimental value.

TABLE 9. CALCULATED REACTIVITY VALUES AND DEVIATION IN PCM FROM STOCHASTIC CALCULATIONS AND EXPERIMENTAL DATA

FA **CR**	**72** **190mm**	**Dev** **(pcm)**	**72** **170mm**	**Dev** **(pcm)**	**72** **151mm**	**Dev** **(pcm)**	**72** **70mm**	**Dev** **(pcm)**
Exp.	**40.0**		**34.0**		**25.0**		**0.0**	
SCK-CEN	-35.0	75.0	-92.1	126.1	-85.1	110.1	-102.1	102.1
VTT-1	330.9	-290.9	319.0	-285.0	313.0	-288.0	286.2	-286.2
VTT-2	363.7	-323.7	354.7	-320.7	344.8	-319.8	317.0	-317.0
CEA	594.4	-554.4	595.4	-561.4	580.6	-555.6	549.0	-549.0
HZDR-1	440.1	-400.1	430.1	-396.1	420.2	-395.2	396.4	-396.4
HZDR-2	9.0	31.0	-0.2	34.2	-4.4	29.4	-35.9	35.9
HZDR-3	91.9	-51.9	83.9	-49.9	76.9	-51.9	48.0	-48.0
HZDR-4	-140.9	180.9	-155.3	189.3	-158.1	183.1	-185.5	185.5
CER	192.6	-152.6	170.7	-136.7	160.7	-135.7	147.8	-147.8
IAEA-1	-11.0	51.0	-21.0	55.0	-25.0	50.0	-56.0	56.0
IAEA-2	-2.0	42.0	-11.0	45.0	-18.0	43.0	-39.0	39.0
IGCAR-1	-208.4	248.4	-215.5	249.5	-220.5	245.5	-249.6	249.6
IGCAR-2	-61.0	101.0	-68.0	102.0	-73.1	98.1	-101.1	101.1
IGCAR-3	----	----	----	----	----	----	275.2	-275.2
IGCAR-4	----	----	----	----	----	----	-461.1	461.1
IGCAR-5	----	----	----	----	----	----	963.6	-963.6
IGCAR-6	----	----	----	----	----	----	826.1	-826.1
NINE-UNIPI	-146.2	186.2	-152.0	186.0	-163.8	188.8	-183.2	183.2
JAEA	211.6	-171.6	215.5	-181.5	210.6	-185.6	173.7	-173.7
KAERI	18.0	22.0	5.0	29.0	9.0	16.0	-25.0	25.0
UNIST	74.9	-34.9	71.9	-37.9	63.0	-38.0	44.0	-44.0
ININ	48.0	-8.0	41.0	-7.0	28.0	-3.0	4.0	-4.0
RATEN-1	141.8	-101.8	121.9	-87.9	116.9	-91.9	97.9	-97.9
RATEN-2	129.8	-89.8	118.9	-84.9	112.9	-87.9	87.9	-87.9
IPPE	30.0	10.0	25.0	9.0	17.0	8.0	-8.0	8.0
NRCKI-1	-122.1	162.1	-126.2	160.2	-119.1	144.1	-151.2	151.2
NRCKI-2	70.9	-30.9	48.0	-14.0	35.0	-10.0	-39.0	39.0
VUJE	129.8	-89.8	133.8	-99.8	119.9	-94.9	97.9	-97.9
USNRC	-57.3	97.3	-88.7	122.7	-88.5	113.5	-106.2	106.2
CIAE	159.7	-119.7	172.7	-138.7	146.8	-121.8	81.9	-81.9
INEST	185.7	-145.7	170.7	-136.7	158.7	-133.7	146.8	-146.8

In the case of Stochastic codes, it is also possible to group results as a function of XS's Data file used, thus, based on Table 5, participant's results were grouped. Figure 9 presents a comparison of average value of calculated results with same evaluated data file used.

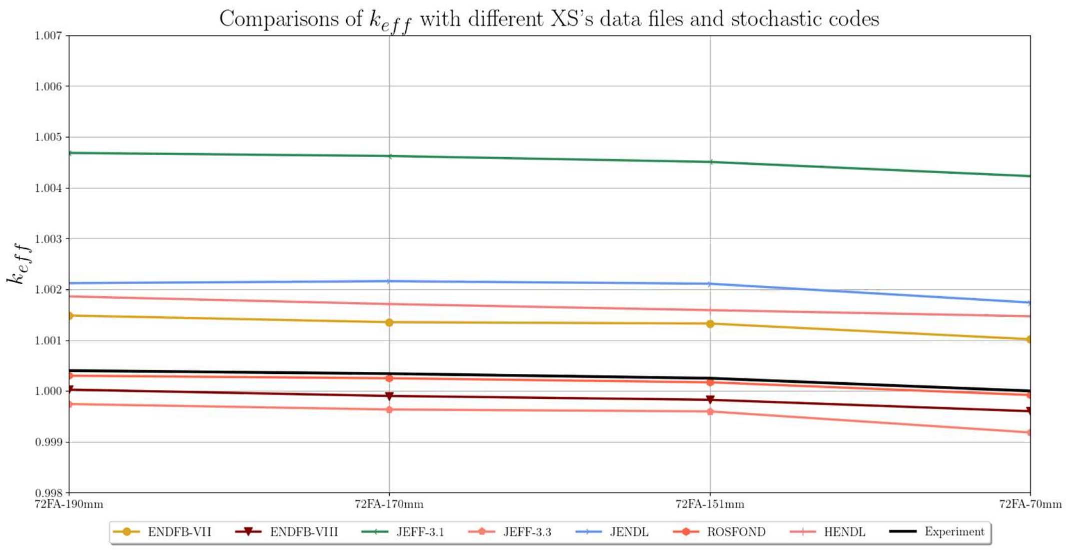

FIGURE 9. EXPERIMENTAL VALUES AND EXPECTED OUTPUT WITH STOCHASTIC CODES IN THE REFINED PHASE

6. CONCLUSIONS

As expected, all refined results presented improvements in the comparisons against experiment values. Also, due to the solving method and to the geometry details and continuous energy on Monte Carlo codes, calculations with Stochastic codes behaved, in general, better than deterministic codes.

In the case of deterministic codes, deviations from average value in the blind phase calculation ranked from -900 to +1000 pcms, almost 2,000 pcms of difference in the more extreme cases. The reason of this large deviation range is the very different numerical approaches implemented in the deterministic solvers going from pure diffusion in some cases to more complex transport solvers in other cases. Calculations were produced with 18 different codes in both phases. As expected, higher differences were found in codes based on diffusion approximation. For the refined phase, adjusts not only in the model but also in the generation of XS's and in some cases further developments in the numerical solvers resulted in significant improvement in calculations. Average of absolute value of deviation from all participant, but in this case against experimental values, was only 320 pcm's.

For Stochastic codes, in the blind phase, deviation from average value was significantly lower than with deterministic codes, since all Monte Carlo codes have the same foundations, in this case, 10 different Monte Carlo codes were used, being Serpent the one used by most of the participants (11 out of 20 participants). The deviation in pcm from average values ranked in ±400 pcm (800 pcms in the most extreme cases) with just some exceptions with over 600 pcms as an absolute value for the homogeneous models. In the refined phase, as in the deterministic calculations, significant improvement was obtained in calculations. Average of absolute value of deviation from all participants was only 167 pcms. In the case of Stochastic codes, the improvements come directly from model adjustments, contrary to deterministic codes in which there are much more variables that can be adjusted: model, XS's generation, numerical solver, etc.

Although stochastic results are more accurate, it is more notorious the improvement on refined phase in the case of deterministic codes. Table 10 shows the mean absolute deviation value from experiment of all calculations for the blind and refined phase with deterministic and stochastic codes.

TABLE 10. MEAN ABSOLUTE DEVIATION VALUE FROM EXPERIMENT OF ALL CALCULATIONS FOR THE BLIND AND REFINED PHASE

	Blind phase	Refined phase	Improvement
Deterministic codes	448 pcm	320 pcm	128 pcm
Stochastic codes	224 pcm	167 pcm	57 pcm

ACKNOWLEDGEMENTS

The data and information presented in the paper are part of an ongoing IAEA coordinated research project on "Neutronics Benchmark of CEFR Start-Up Tests – CRP-I31032.

REFERENCES

[1] HUO, XINGKAI, "Technical Specifications for Neutronics Benchmark of CEFR Start-up Tests, Version 7.0," KY-IAEA-CEFRCRP-001, China Institute of Atomic Energy, December 2019.